ORIGINAL ARTICLE

Pure redox-sensitive paclitaxel−maleimide prodrug nanoparticles: Endogenous albumin-induced size switching and improved antitumor efficiency

Xinyu Lou[a,†], Dong Zhang[b,c,†], Hao Ling[b], Zhonggui He[b], Jin Sun[b], Mengchi Sun[b,*], Dongchun Liu[a,*]

[a]School of Traditional Chinese Materia Medica, Shenyang Pharmaceutical University, Shenyang 110016, China
[b]Wuya College of Innovation, Shenyang Pharmaceutical University, Shenyang 110016, China
[c]Jiangsu Hengrui Medicine Co., Ltd., Lianyungang Eco & Tech Development Zone, Lianyungang 222047, China

Abstract A commercial albumin-bound paclitaxel nano-formulation has been considered a gold standard against breast cancer. However, its application still restricted unfavorable pharmacokinetics and the immunogenicity of exogenous albumin carrier. Herein, we report an albumin-bound tumor redox-responsive paclitaxel prodrugs nano-delivery strategy. Using diverse linkages (thioether bond and disulfide bond), paclitaxel (PTX) was conjugated with an albumin-binding maleimide (MAL) functional group. These pure PTX prodrugs could self-assemble to form uniform and spherical nanoparticles (NPs) in aqueous solution without any excipients. By immediately binding to blood circulating albumin after intravenous administration, NPs are rapidly disintegrated into small prodrug/albumin nanoaggregates in vivo, facilitating PTX prodrugs accumulation in the tumor region via albumin receptor-mediated active targeting. The tumor redox dual-responsive drug release property of prodrugs improves the selectivity of cytotoxicity between normal and cancer cells. Moreover, disulfide bond-containing prodrug/albumin nanoaggregates exhibit long circulation time and superior antitumor efficacy in vivo. This simple and facile strategy integrates the biomimetic characteristic of albumin, tumor redox-responsive

---

on-demand drug release, and provides new opportunities for the development of the high-efficiency anti-tumor nanomedicines.

1. Introduction

Cancer is one of the most lethal diseases with high mortality around the world[1]. The chemotherapy, a common cancer treatment modality, has achieved considerable success[2]. However, the main obstacles to the treatment efficacy of chemotherapy stem from the poor solubility, nonspecific distribution, and severe toxicity of chemotherapeutic drugs[3]. To address these challenges, great efforts have been developed to enhance chemotherapeutic drugs-mediated anticancer responses[4,5]. Among them, the prodrug-based nano-drug delivery systems (nano-DDSs), which integrate the advantages of prodrugs and nano-DDS, show more distinctive advantages such as high drug loading, limited excipient-associated toxicity and tumor-targeting characteristic *via* enhanced permeability and retention (EPR) effect[6−9]. Nevertheless, due to dense tumor matrix and high interstitial pressure, the large nano-size cannot be able to deeply penetrate into tumor core, resulting in compromised therapeutic effect.

Albumin, the most abundant protein in plasma (35−50 mg/mL), has been extensively studied among nano-sized drug carriers due to its high stability, long circulatory half-life (19 days) and albumin-mediated tumor-penetrating effect[10,11]. For example, the albumin-bound paclitaxel nanoparticle (Abraxane) has demonstrated remarkable promise of an albumin-based nanovector application for cancer therapy[12]. However, tedious purification process, rapid clearance upon intravenous infusion and immunogenicity limited its further availability and applicability in clinic[13]. Given the selective conjugation of maleimide group with the cysteine-34 residue of albumin *in situ*[14], we have established a series of albumin-bound paclitaxel−maleimide prodrug nanoparticles (NPs) with the addition of polymer DSPE−PEG$_{2K}$. The study found that the introduction of long-chain PEG remained the great colloidal stability of NPs, but impaired the cellular uptake and accelerated blood clearance (ABC) phenomenon[15,16].

To further exploit the excipient-free delivery against cancer, we herein reported albumin-induced transformative nanomedicines of paclitaxel (PTX) prodrugs NPs by binding to plasma albumin to improve tumor-targeting drug delivery. We constructed the redox-responsive paclitaxel−maleimide prodrugs NPs using thioether bond (PSMAL), disulfide bond (PSSMAL) as linkages without any excipients. The paclitaxel−maleimide (PMAL) and succinimide−paclitaxel (PSUC) prodrugs NPs were also prepared as negative control. Following intravenous injection, plasma albumin can promote to convert large paclitaxel−maleimide prodrugs NPs to small prodrug/albumin nanoaggregates *in vivo*. Further, tumor microenvironment-responsive PTX prodrugs could selectively release the active PTX molecules, resulting in the enhanced antitumor activity. This work presents a novel design strategy of the high-efficiency anti-tumor nanomedicines, which combines the albumin-mediated tumor targeting with the redox-sensitive prodrug-based DDSs.

2. Materials and methods

2.1. Materials

PTX prodrug was synthesized according to our previously reported protocol. Commercial preparation Taxol® was purchased from Birstol-Myers Squibb Trading Co., Ltd. (Shanghai China). 6-Maleimidocaproic acid (EMC) was obtained from Energy Chemical (Shanghai, China). Amplite™ colorimetric maleimide quantitation kit was purchased from Dakewe Biotech Co., Ltd. (Beijing, China). Hydrogen peroxide solution (H$_2$O$_2$) and D,L-dithiothreitol (DTT) were supplied by Aladdin Biochemical Technology Co., Ltd. (Shanghai, China). Bovine serum albumin (BSA) was purchased from HarveyBioGene Technology Co., Ltd. (Beijing, China). Murine mammary carcinoma cells (4T1), oral squamous cell carcinoma cells (KB) and murine embryo fibroblast cells (NIH/3T3) were obtained from American Type Culture Collection (ATCC). Fetal bovine serum (FBS) was obtained from Hyclone (Beijing, China). Cell culture media, penicillin-streptomycin and MTT were provided by GIBCO (CA, USA). All other reagents and solvents applied in this study were of analytical or HPLC grade.

2.2. Preparation and characterization of PTX prodrug nanoparticles (NPs)

PTX prodrug nanoparticles were prepared by nanoprecipitation method. In brief, 4 mg of PTX prodrugs (PMAL, PSUC, PSMAL, and PSSMAL) were dissolved in 1 mL of anhydrous ethanol-THF (9:1, *v/v*) mixed solvent. Next, the solution was added dropwise to 4 mL of deionized water. After agitating for 1 min, the PTX prodrug nanoparticles were formed randomly. The remaining organic solvent was removed by rotatory evaporation at 37 °C and the retained NPs were further dispersed with deionized water to acquire the final prodrug NPs (1 mg/mL).

Additionally, the morphology of PTX prodrug nanoparticles was observed using transmission electron microscope (TEM, Hitachi, H-600, Tokyo, Japan). Negative staining method was applied to preparing TEM samples. Briefly, a drop of nanoparticle solution was dripped on the copper mesh. When the solvent was completely evaporated, the sample was negatively stained by 2% phosphotungstic acid for 20 min and dried naturally. The sample was then imaged by TEM.

2.3. Quantification of maleimide groups on PTX prodrug NPs

Amplite™ colorimetric maleimide quantitation kit was used for maleimide quantification. According to the assay protocol, 40 μL of MEA (GSH) was added to 160 μL of deionized water or prodrug NPs (0.25 mg/mL). After incubated at ambient temperature for 20 min, the absorbances of these samples were determined at 324 nm signed as OD$_0$' or OD$_0$, respectively. Then 4 μL of 50X 4,4′-dithiodipyridine (4,4′-DTDP) stock solution was added to the
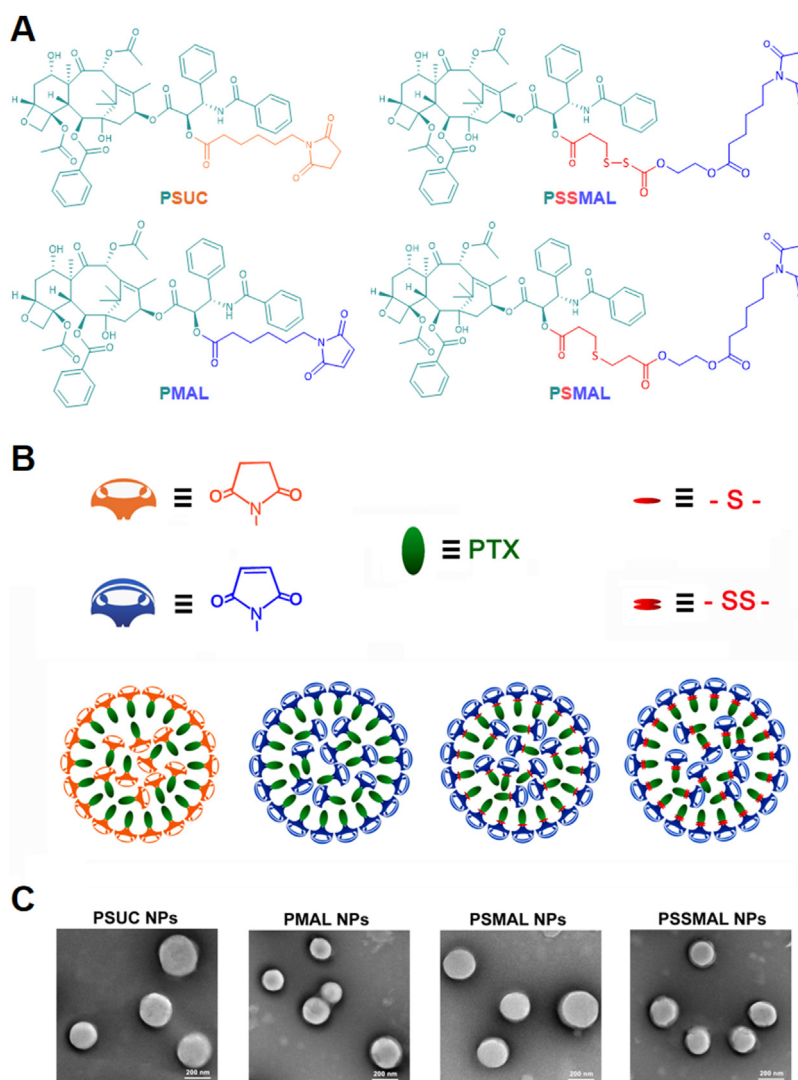
Figure 1 (A) Chemical structures of four PTX prodrugs. (B) Schematic illustration of the preparation of prodrug nanoparticles. (C) TEM images of PTX prodrug nanoparticles. Scale bar = 200 nm.

samples and incubated at room temperature for 2 min. The absorbances of the samples at 324 nm was measured again as OD_{TSH} or OD. The measurement was performed on Microplate Reader (BioRed, Model 500, CA, USA). The mol% of maleimide was calculated, as shown in Eqs. (1) and (2):

$$\Delta OD = \left(OD_{TSH} - OD_0'\right) - \left(OD - OD_0\right) \qquad (1)$$

Mol% of maleimide = ΔOD

$\times$ sample volume/coefficient of DTDP/moles of prodrug

$\times 100$ (2)

2.4. Albumin-binding property of PTX prodrugs

To evaluate whether the maleimide moiety could covalently bind to albumin, HPLC was performed to determine the content of non-binded PTX prodrug after an incubation with BSA solution. Briefly, 0.5 mL of PTX prodrug (0.2 mg/mL) was added to 0.5 mL excessive amount of BSA solution (4 mg/mL) and incubated at

37 °C for 2 or 60 min. Besides, for blocking study, equivalent BSA solution was preincubated with excess EMC for 30 min and further incubated with PTX prodrug for 60 min. All the samples were analyzed with HPLC (Hitachi HPLC system, Tokyo, Japan).

The separation was achieved on a Waters Symmetry 300™ C18 column (250 mm × 4.6 mm, 5 μm) at 35 °C with a mobile phase consisted of water containing 0.1% trifluoroacetic acid (mobile phase A) and acetonitrile containing 0.1% trifluoroacetic acid (mobile phase B) at a flow rate of 1.0 mL/min. The gradient elution procedure was applied as follows: 0−5 min 95% A, 5−30 min 95%−60% A, 30−45 min 60% A, 45−80 min 60%−50% A, 80−85 min 50%−95% A, 85−90 min 95% A. Peaks were monitored at 230 nm.

2.5. Molecular docking

Binding of PTX prodrugs to serum albumin was investigated by means of molecular docking. The structures of PTX prodrugs were created using Msketch software (ChemAxon, Maevin Sketch 16.4.25.0, Budapest, Hungary) and defined as the ligands. The
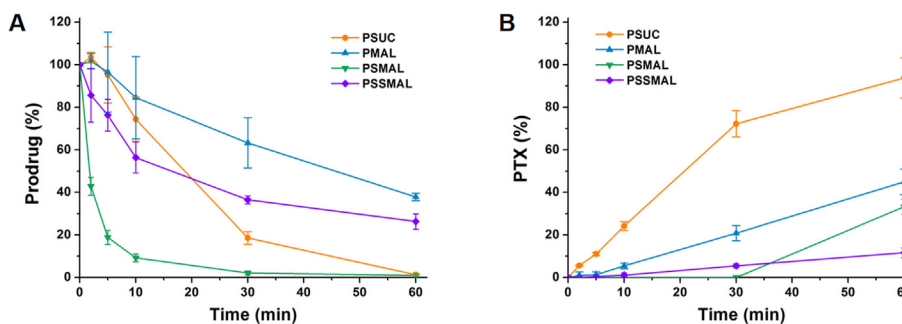
Figure 2   Chemical stability of PTX prodrugs. Cumulative release of (A) prodrug and (B) PTX after incubation in rat plasma.

crystal structure of BSA (PDB ID:3V03) was retrieved from Protein Data Bank (http://www.rcsb.org), which was defined as the receptor. The proteins were prepared by using Protein Preparation Wizard, including adding Hydrogen atoms, removing water molecules and distributing local ions. Finally, the protein was optimized with OPLS_2005 force field until the root mean square deviation value below 0.30 A. Ligand structures were optimized using Ligprep module, and minimized with OPLS 2005 force field. As a next step, the docking study was performed by using Glide module embedded in the Schröinger Maestro interface.

2.6.   Stability of PTX prodrug nanoparticles in different media

The colloidal stability of PTX prodrug nanoparticles was assessed in the presence of rat plasma and 20 mg/mL BSA (1:3, v/v) with the stirring speed of 100 rpm at 37 °C (Anting, TGL-16B, Shanghai, China). After incubation, the mean diameter of PTX prodrug nanoparticles was measured by Nano ZS Zetasizer (Malvern, Malvern, UK) at 0, 2, 4, 8, 12, and 24 h. Additionally, to investigate the long-term stability of nanoparticles, the NPs were stored at 4 °C for 10 days. The particle size was used as stability indicator.

2.7.   Stability of PTX prodrugs in plasma

The stability of PTX prodrugs in rat plasma was also evaluated. The fresh whole blood was collected from Sprague−Dawley (SD) rats orbit and was centrifuged at 3500 rpm (Anting) for 10 min to obtain fresh plasma. For the detection of PTX prodrug, plasma was pre-incubated with an excess of EMC at 37 °C for 30 min. Then the plasma was incubated with appropriate amount of prodrugs for 60 min. At the designed time intervals, 50 μL samples were withdrawn and added 150 μL acetonitrile to deproteinize the plasma. Subsequently, the sample was centrifuged at the speed of 13,000 rpm (Anting) for 10 min and 10 μL supernatants were analyzed by HPLC (Hitachi). The residual prodrug and released PTX were also measured.

2.8.   Redox-responsive release behavior of PTX prodrugs

To estimate the redox sensitivity of drug release, PTX release was conducted in ethanol-containing PBS [30% ethanol (v/v), pH 7.4] with different concentrations of H_2O_2 and DTT. Typically, appropriate volume of PTX prodrugs were dispersed in 30 mL releasing mediator, then incubated at 37 °C with the shaking speed of 100 rpm (Anting). At pre-determined intervals, samples were withdrawn and replaced by corresponding fresh medium. The concentration of released PTX was determined by HPLC

(Hitachi). The analysis was performed on an ODS C18 column (250 mm × 4.6 mm, 5 μm) using water/acetonitrile (40:60, v/v) as mobile phase at the flow rate of 1 mL/min with a temperature of 35 °C. The analytical wavelength was 227 nm.

2.9.   In vitro cytotoxicity assays

The cytotoxicity of Taxol® and prodrug nanoparticles was evaluated by MTT assay in KB, 4T1 and NIH/3T3 cells. In brief, cells were seeded in 96-well plates at a density of 2×10^4 cells/mL and cultured for 24 h. Afterwards, the culture medium was removed, and the cells were treated with 200uL gradient concentrations of Taxol® or prodrug NPs for 48 or 72 h. All concentrations were carried out in triplicate. Cells cultured in 200 μL culture medium, served as negative control. Then, the medium was replaced with 200 μL fresh culture medium containing 20 μL MTT solution (5 mg/mL). After 3 h incubation, the medium containing unreacted MTT was discarded. The obtained violet formazan precipitate was dissolved in 200 μL of DMSO, and the absorbance was measured at a wavelength of 490 or 570 nm by means of a BioRadicroplate reader (BioRed). The IC_{50} values were calculated with SPSS software.

2.10.   Intracellular PTX release

To quantitatively determine the intracellular PTX released from prodrug nanoparticles, 4T1 or NIH/3T3 cells were cultured in 24-well plates at a density of 1×10^5 cells per well for 24 h. Subsequently, the culture medium was removed and replaced with medium containing various concentrations of PTX nanoparticles (PTX equivalent concentrations: 200, 400 and 800 ng/mL) for 4 or 24 h. Then, cells along with the drug-containing culture medium were collected, and broken by ultrasonication. After centrifugation at 13,000 rpm for 5 min (Anting), the supernatant was obtained and frozen at −20 °C for further analysis.

The protein was precipitated by methanol, and the concentrations of released PTX in the supernatant were analyzed by UPLC−MS/ MS (Waters, Milford, USA) with diazepam as internal standard (IS). A BEH C18 column (50 mm × 2.1 mm, 1.7 μm) was used for chromatographic separation. The mobile phase was composed of water containing 0.1% formic acid (solvent A) and acetonitrile (solvent B) at a gradient elution of 0−1.0 min, 70% A; 1.1−3.0 min, 15% A; 3.1−4.0 min, 70% A. The column temperature was maintained at 40 °C with a flow rate of 0.2 mL/min. Mass spectrometry analysis was carried out using triple quadruple detector equipped with an ESI in positive ionization mode. The collision energy of PTX and diazepam was set at 30 and 27 V, respectively. The operating parameters were set as follows: capillary voltage, 3.5 kV;
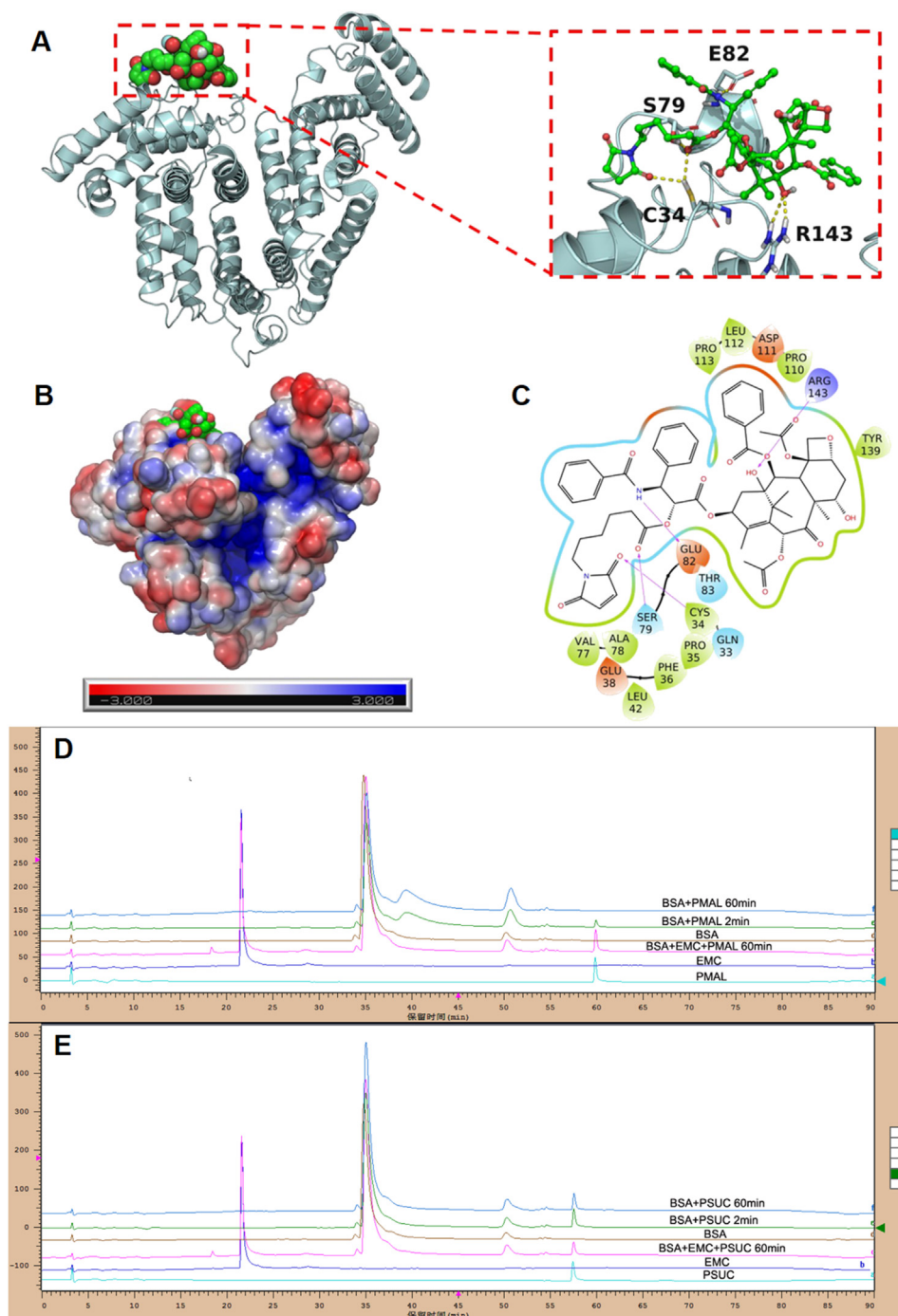
Figure 3 (A) Binding diagram between PMAL and albumin. (B) The electrostatic potential surface of albumin. (C) The two-dimension (2D) binding interactions between PMAL and albumin. Albumin binding studies of PTX prodrugs NPs. HPLC spectra of (D) PMAL and (E) PSUC prodrug before or after incubation with BSA.

cone voltage, 50 V; desolvent temperature, 350 °C; desolvent flow rate, 650 L/h; scan duration, 0.2 s. Multiple reaction monitoring (MRM) was used to monitor the transition of m/z 876.6 [M+Na]$^+$ → 308.2 and m/z 284.8 [M+H]$^+$ → 193.0, respectively.

2.11. Animals

Sprague−Dawley rat (180−220 g) and BALB/c female mice (18−22 g) were supplied by the Laboratory Animal Center of Shenyang Pharmaceutical University (Shenyang, China). All

experimental procedures were executed according to the protocols approved by Shenyang Pharmaceutical University Animal Care and Use Committee, Shenyang, China.

2.12. In vivo antitumor efficacy

The therapeutic efficacy of PTX prodrug nanoparticles was evaluated in the breast cancer female BALB/c mice model. To establish the breast cancer model, 4T1 cells were suspended in PBS (5 × 10^6 cells/mL) and subcutaneously injected into the

left back at a dose of about 100 μL per mouse. When tumor volumes reached around 100 mm^3, the mice were randomly assigned into six groups with 5 mice per group. Then, PBS (pH = 7.4), Taxol$^®$ and PTX prodrug nanoparticles was intravenously injected (8 mg PTX per kg body weight) at a 2-day interval for five times. The tumor volume and body weight of each mouse were monitored every other day. The tumor volume was calculated as shown in Eq. (3):

$$V = W^2 \times L/2 \tag{3}$$

where W and L represented the shortest and longest diameters of the tumor, respectively.

2.13. Pharmacokinetics

4T1 xenograft tumor-bearing BALB/c mice were used to investigate the pharmacokinetic profiles of prodrug nanoparticles. The mice were randomly divided into three groups and were intravenously administrated Taxol, PMAL NPs and PSSMAL NPs at an equivalent PTX dose of 4 mg/kg. At the designed time intervals, about 300 μL blood were collected, centrifuged and stored at −80 °C until analysis. The plasma concentration of free PTX was analyzed by UPLC−MS/MS (Waters).

2.14. Biodistribution

The *in vivo* biodistribution of Taxol and PTX prodrugs nanoparticles were performed by 4T1 tumor-bearing BALB/c mice. For this, 4T1 cells were subcutaneously injected into the left flank region of female BALB/C mice. When tumor volumes reached around 200 mm^3, PMAL NPs, PSSMAL NPs and Taxol were injected intravenously *via* tail veil at the equivalence of 4 mg/kg PTX. Then the mice were sacrificed at 6 and 24 h post injection and their major organs as well as tumors were excised, weighed and stored at −20 °C until analysis. The PTX concentrations in

these samples were measured by a UPLC−MS/MS system (Waters).

2.15. Statistical analysis

All data were expressed as mean ± standard deviation (SD). Student's *t*-test was performed to determine differences between groups. The P value of <0.05 is deemed statistically significant.

3. Results and discussion

3.1. Preparation and characterization of PTX prodrug nanoparticles (NPs)

Redox-sensitive PTX−maleimide prodrugs (PSMAL and PSSMAL) were prepared by conjugating maleimide to PTX *via* thioether bond (−S−) and disulfide bond (−S−S−) as previously reported (Fig. 1A)[16], respectively. The ester bond prodrug (PMAL) was designed as a non-sensitive control. Meanwhile, the succinimide−paclitaxel prodrug (PSUC) was also fabricated to verify the function of maleimide moiety[16]. Pure PTX prodrug NPs could be prepared using one-step nanoprecipitation method without any excipients (Fig. 1B). The transmission electron microscopy (TEM) image demonstrated that the prepared prodrugs NPs had a uniform spherical morphology with a diameter of ∼200 nm (Fig. 1C).

3.2. Stability of PTX prodrug NPs

In case of no excipients, the hydrophobic PTX prodrugs could spontaneously self-assemble into NPs with uniform size distribution. Dynamic light scattering (DLS) displayed the hydrodynamic diameters (PMAL: 176.6 ± 7.3 nm; PSUC: 187.4 ± 16.1; PSMAL: 200.1 ± 2.1 nm; PSSMAL: 185.5 ± 10.3 nm). As shown
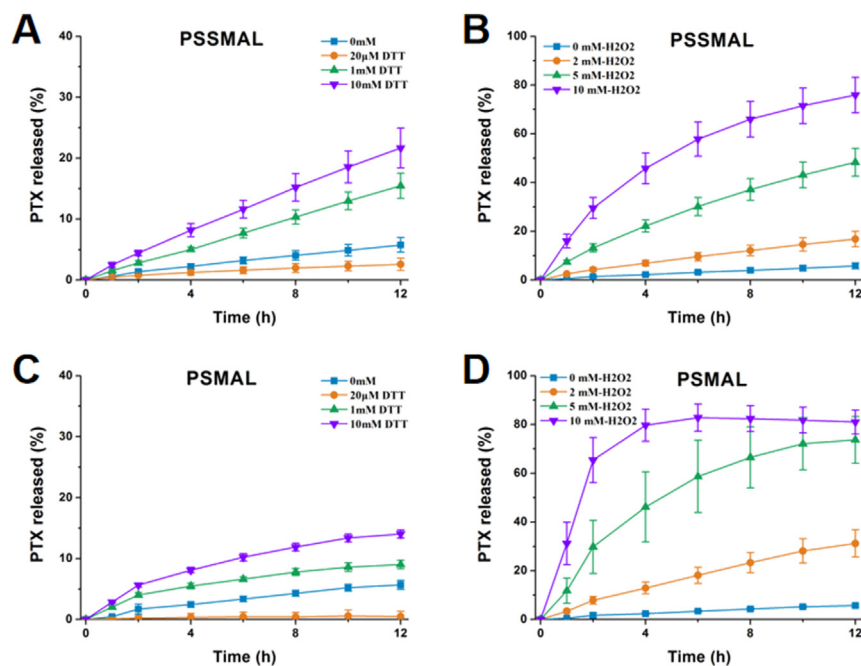
Figure 4 *In vitro* PTX release (%) from (A) PSMAL or (B) PSSMAL in the presence of various concentrations of DTT. PTX release from (C) PSMAL or (D) PSSMAL in the presence of various concentrations of H$_2$O$_2$.
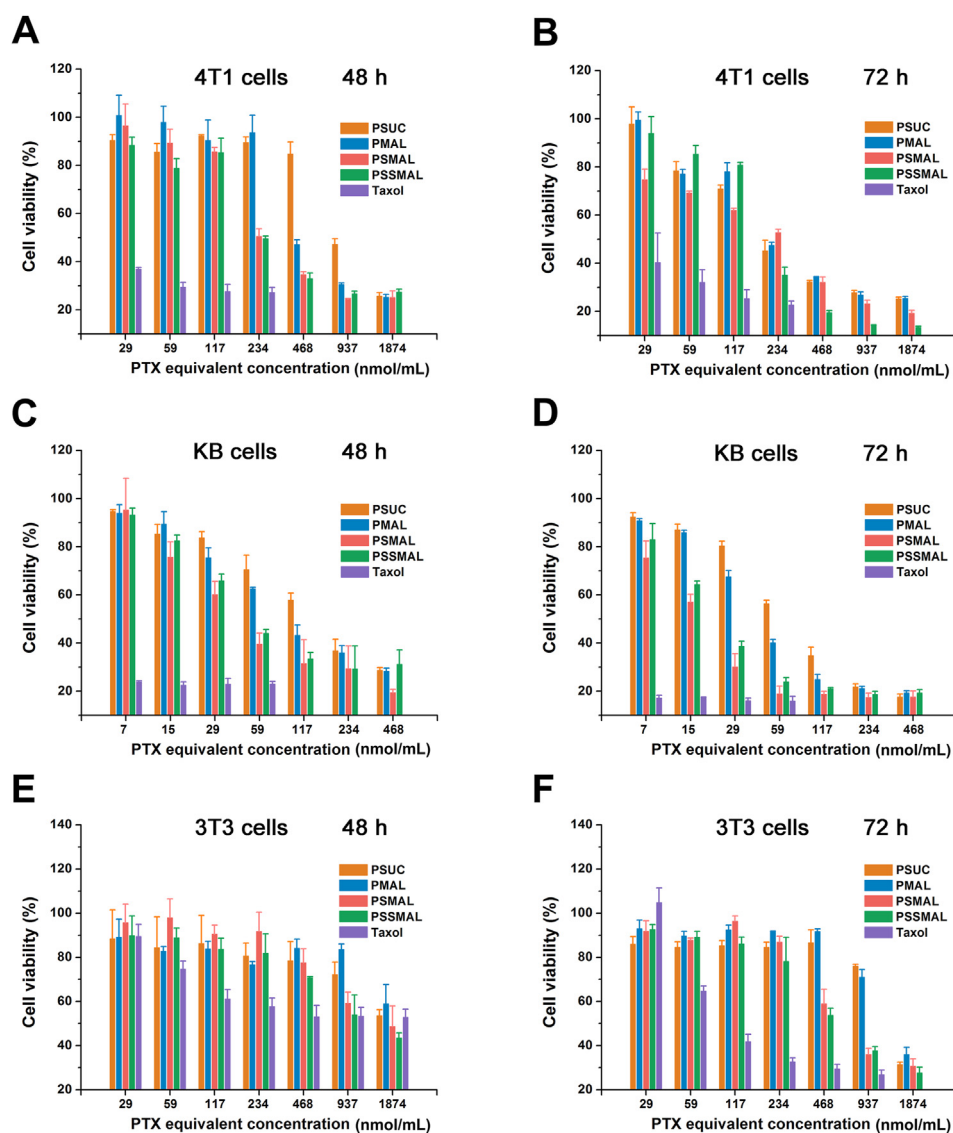
Figure 5   The cytotoxicity of different concentrations of Taxol® and PTX prodrug nanoparticles against 4T1 cells (A and B), KB cells (C and D) and NIH/3T3 cells (E and F) *in vitro* for 48 or 72 h.

in Supporting Information Fig. S1, the hydrodynamic size of NPs stored in 4 °C remained almost unchanged during 10 days, demonstrating the favorable colloidal stability of PTX prodrug NPs in solution.

The chemical stability of PTX prodrugs in rat plasma was also investigated though monitoring concentrations of the residual prodrug and released PTX at various times. The PTX−maleimide prodrugs exhibited higher stability in rat plasma than PSUC due to protective effect of the plasma albumin. Compared with other prodrugs, PTX release from PSSMAL was scarcely detected (<10%) after incubation for 1 h (Fig. 2A and B). These results demonstrated the good chemical stability of PSSMAL in rat plasma.

3.3.   Albumin-binding property of PTX prodrug NPs

Albumin, the most abundant in plasma, is used to deliver the different endogenous and exogenous substances *in vivo*. The fast-replicating cancer cells need substantial nutritional stores *via*

supply of albumin. The albumin specifically accumulates in the tumor tissues due to overexpressed albumin-binding receptors. Inspired by the fact that albumin serves as the great carrier *in vivo*, we explored the albumin-binding capacity of different PTX prodrugs NPs. It was found that the hydrodynamic sizes of PTX−maleimide prodrug NPs dramatically reduced to ∼10 nm upon exposure to the albumin solution (Supporting Information Fig. S2), similar with the size of albumin itself. Except for maleimide-based prodrug NPs, this phenomenon was also reported in sulfonatophenoxyl- and evans blue-based NPs[17,18]. The interaction between albumin and PMAL prodrug was investigated using covalently molecular docking models. As shown in Fig. 3A and C, various hydrogen bonds restricted the stable conformation of PMAL prodrug molecules from free rotating. The resulting albumin/PTX−maleimide prodrug nanoaggregates were further studied by a series of experiments. One key feature of albumin binding ability is the exposed maleimide groups on the prepared NPs surfaces. According to our previous studies, the maleimide groups could covalently conjugate with 34′-cysteine of plasma albumin through
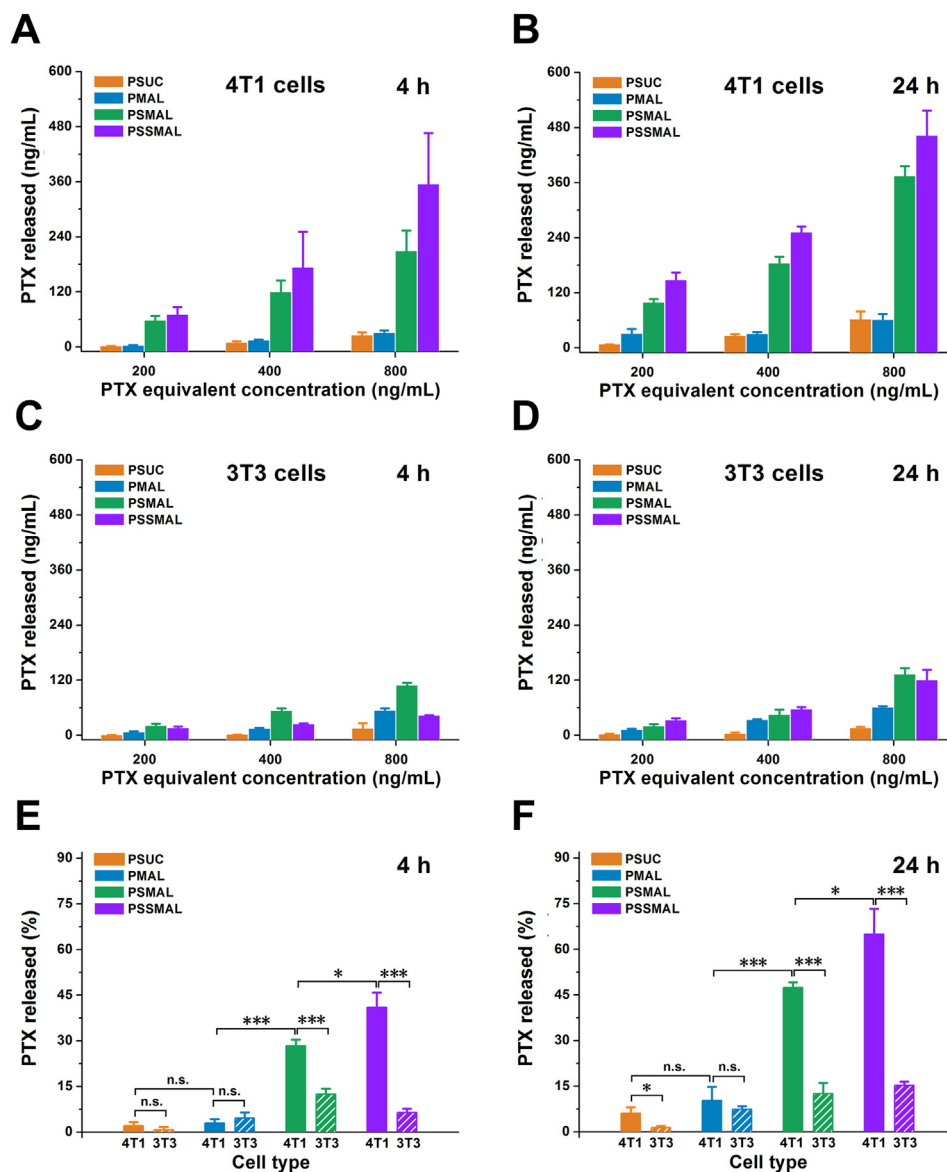
Figure 6 Free PTX level released from the nanoparticles in (A and B) 4T1 cells and (C and D) 3T3 cells for 4 or 24 h. The mean intracellular PTX release in 4T1 cells for (E) 4 or (F) 24 h, compared with the same nanoparticles incubation with 3T3 cells at the same time-point. Data are presented as mean ± SD ($n = 3$). n.s., not significant, $*P < 0.05$, $**P < 0.01$, $***P < 0.001$.

classical thiol−maleimide reactions[15]. As shown in Supporting Information Fig. S3, a few amounts of maleimide groups could be detected on the surface of PSUC. The maleimide contents on the surface of PTX−maleimide prodrug NPs were significantly higher than that of PSUC. Due to the structural flexibility of thioether bond and disulfide bond, maleimide contents on the surface of PSMAL and PSSMAL were much higher than other NPs[16].

Next, the BSA-binding capacity of PTX−maleimide prodrug (PMAL) was evaluated using HPLC method (Fig. 2D and E). PMAL showed strong BSA binding ability. About 80% PMAL prodrugs were bound to BSA within 2 min, and the conjugation process was almost accomplished after incubation for 60 min. Moreover, when the sulfydryl groups of BSA were depleted by 6-maleimidocaproic acid (EMC), PMAL was incapable of conjugating with BSA. It showed no significant changes in PSUC concentration within 60 min incubation, whether the sulfydryl of

BSA existed or not. Based on these results, we confirmed that albumin rapidly trapped the maleimide groups from PTX−maleimide prodrugs and induced the disassembly of PTX−maleimide prodrugs NPs, resulting in the formation of small prodrug/albumin nanoaggregates.

3.4. Redox-responsive release behavior of PTX prodrugs

We next investigated the redox-triggered PTX release performance of PSMAL and PSSMAL prodrugs in PBS containing different concentrations of H_2O_2 (ROS simulatant) and DTT (GSH simulatant) environment. The release of PTX from PMAL and PSUC prodrugs in PBS with 10 mmol/L H_2O_2 was measured as negative controls. As shown in Fig. 4, all prodrugs were stable in PBS and a few release of PTX ($<10\%$) was observed over 12 h. With increasing concentrations of H_2O_2, the percentage of PTX
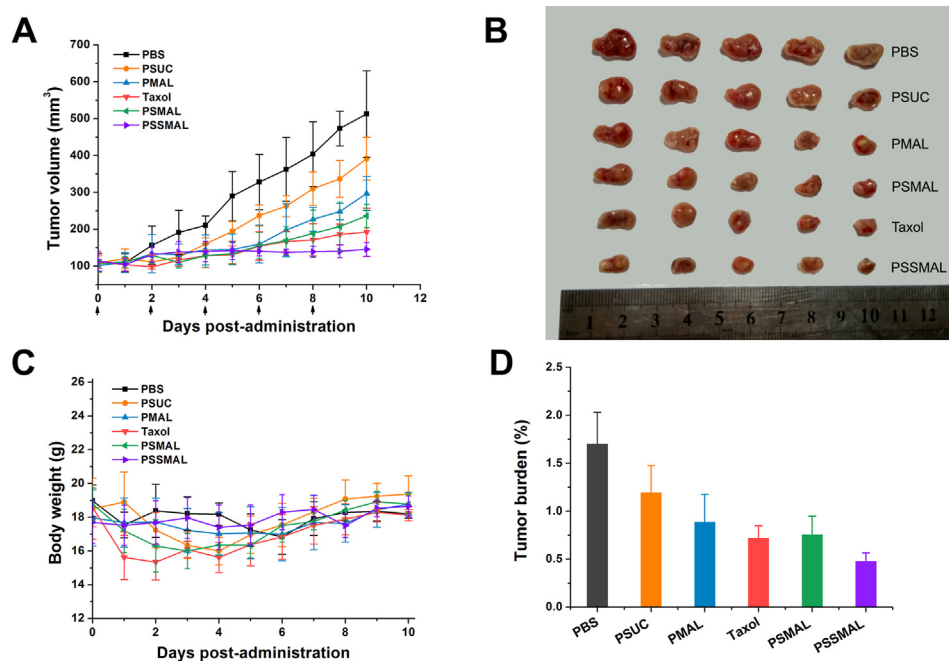
Figure 7 *In vivo* antitumor efficacy of the PTX prodrug nanoparticles against 4T1 ectopic tumors. (A) Tumor growth curves of mice treated with different preparations. (B) The image of tumors at the end of the treatment. (C) Tumor burden after last treatment. (D)The changes of body weight.
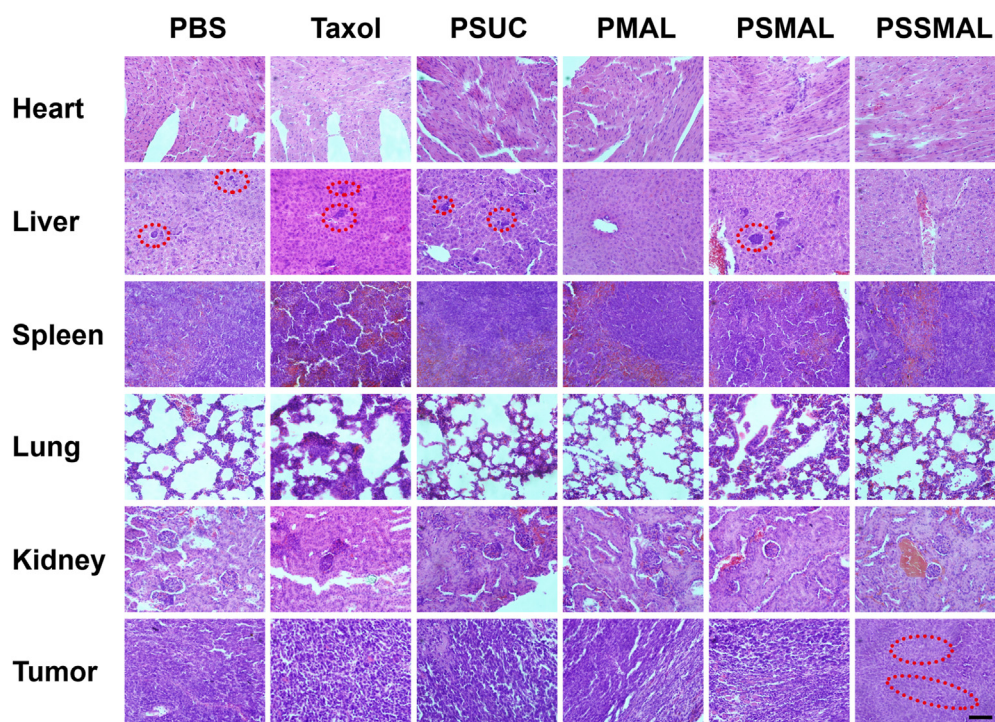
Figure 8 H&E-stained slices of major organs and tumors from mice receiving different treatments. The red circles indicated the metastatic tumor. Scale bar = 100 μm.

released from PSMAL and PSSMAL gradually increased. The released amount of PTX reached up to 80% in the presence of 10 mmol/L H_2O_2, confirming that the thioether bond and disulfide bond were readily decomposed by H_2O_2. The PSMAL exhibited faster oxidation-triggered PTX release than PSSMAL.

Furthermore, with increasing concentrations of DTT, the percentage of PTX released from PSMAL and PSSMAL gradually increased. The PSSMAL exhibited a more rapid release characteristic under the reduction condition than PSMAL. As expected, the other two non-sensitive prodrugs (PMAL and PSUC) showed

quite slow drug release rate in PBS with or without H_2O_2 (Fig. 4). These observations revealed that PSMAL and PSSMAL prodrugs could be relatively stable in the normal tissue, while PTX could be rapidly released in the redox microenvironment of tumor cells.

3.5. In vitro cytotoxicity assays

The *in vitro* cytotoxicity of PTX prodrug NPs and Taxol® was assessed by the MTT assay. As shown in Fig. 5, PTX prodrugs NPs exhibited a concentration-dependent cytotoxicity. All prodrugs NPs were less effective in killing tumor cells than Taxol® because of the delayed release and bioactivation of the cytotoxic PTX molecules. Among these, both PSMAL and PSSMAL NPs showed higher cytotoxicity ability than PMAL and PSUC due to the tumor redox-responsive drug release. Compared to Taxol®, normal cells (3T3) treated with PSMAL and PSSMAL retained high viabilities with concentration ranging from 59 to 234 nmol/L, indicating that PSMAL and PSSMAL had the selective cytotoxicities between normal cells and cancer cells.

3.6. Intracellular PTX release

Motivated by the differential cytotoxicities between tumor and normal cells, we further evaluated the intracellular release of PTX from PTX prodrugs NPs in 4T1 and 3T3 cells. The results in Fig. 6 revealed that PSMAL and PSSMAL showed a concentration-dependent PTX release in 4T1 and 3T3 cells regardless of the incubation time. The PTX release efficiency of the PSMAL and PSSMAL in 4T1 cells was much higher than 3T3 cells. The similar PTX amounts were released from PSUC and PMAL in 4T1 and 3T3 cells. The results of intracellular PTX release were consistent with that of *in vitro* cytotoxicity. This confirmed that PSMAL and PSSMAL showed hyper-selective release of PTX towards cancer cells and normal cells.

3.7. In vivo anticancer efficacy

The influence of *in situ* albumin-immobilized prodrugs on pharmacokinetics was investigated by intravenously injecting Taxol, PMAL and PSSMAL into 4T1 xenograft tumor-bearing BALB/c mice at an equivalent PTX dose of 4 mg/kg. As shown in Supporting Information Fig. S4A, free PTX from Taxol were rapidly cleared from the blood owing to its short half-life. By contrast, PMAL and PSSMAL could prolong the blood circulation. Notably, compared to PMAL, the released PTX from PSSMAL exhibited a long blood circulation time, which would be beneficial to increase the tumor accumulation of PTX through the EPR effect.

The *in vivo* biodistribution of prodrug NPs was investigated in nude mice bearing 4T1 tumor. As shown in Figs. S4B and 4C, the *in vivo* PTX concentration results showed that free PTX from PSSMAL exhibited significantly increased concentration in tumor compared to free PTX from PMAL or Taxol at 6 or 24 h, which were well consistent with the above pharmacokinetic assay. And high PTX concentration was detected in lung and tumors treated with both PTX prodrug formulations. To sum up, the long systemic circulation, the EPR effects and redox-sensitive characteristics of PSSMAL greatly facilitated the intratumoral accumulation and release of PTX.

Encouraged by the hyper-selective release of PTX *in vivo*, PTX prodrug NPs and Taxol® were conducted to investigate the antitumor efficacy *in vivo*. The 4T1 tumor-bearing mice were

intravenously administered with different formulations. As depicted in Fig. 7A and C, mice in PBS treatment group experienced a rapid tumor growth to >500 mm³ at the end of treatment. In consistent with the poor *in vitro* cytotoxicity, PSUC displayed moderate tumor growth inhibition. The antitumor effect of PTX–maleimide prodrugs NPs were stronger than PSUC NPs, owing to the tumor accumulation effect of the *in vivo* albumins captured by maleimide groups. Taxol®, PMAL and PSMAL NPs exhibited similar tumor inhibition degrees. Among them, mice treated with PSSMAL NPs demonstrated a prominent antitumor effect and dramatically delayed tumor progression. The potent antitumor efficacy of PSSMAL could be attributed to the favorable plasma stability, high accumulation at the tumor site and efficient tumor redox-responsive drug release.

Additionally, the body weights of the mice were not apparently changed during the treatments, except for Taxol® group. This indicated that PTX prodrugs NPs were safer than Taxol® group (Fig. 7D). As shown in Fig. 8, no noticeable tissue damage was found in the H&E-stained images of tissue sections. The obvious hepatic metastases were observed in PBS, Taxol®, PSUC and PSMAL NPs groups. These results clearly demonstrate that PSSMAL NPs elicited potent antitumor efficacy, reduced side effects, inhibited the liver metastasis and provided an alternative therapy option for breast tumor.

4. Conclusions

Here, we successfully synthesized *in vivo* endogenous albumin-bound PTX–maleimide prodrugs NPs for tumor microenvironment-activated cancer therapy through redox-responsive linkages. The maleimide-obtained NPs can rapidly bind to the plasma albumin and transform into small prodrug/albumin nanoaggregates *in vivo*, thus achieving low immunogenicity and great intra-tumor accumulation. More importantly, both disulfide bond-bridged NPs and thioether bond-bridged NPs (PSSMAL and PSMAL) not only showed the hyper-selective cytotoxicity between tumor and normal cells, but also enhanced the circulation time and tumor inhibition effect in BALB/c mice bearing 4T1 tumor. As a consequence, *in vivo* endogenous albumin-bound prodrug NPs pave the way for designing targeted delivery nano-platform for tumor therapy.

Author contributions

Dong Zhang carried out the experiments and performed data analysis. Xinyu Lou and Linghao participated part of the experiments. Zhonggui He provided experimental drugs and quality control. Mengchi Sun and Xinyu Lou wrote the manuscript. Jin Sun and Dongchun Liu revised the manuscript. All of the authors have read and approved the final manuscript.

Conflicts of interest

The authors have no conflicts of interest to declare.

Appendix A.   Supporting information

Supporting data to this article can be found online at https://doi. org/10.1016/j.apsb.2020.12.001.

References

1. Siegel RL, Miller KD, Jemal A. Cancer statistics 2017. *Ca Cancer J Clin* 2017;**67**:7−30.
2. Wan X, Beaudoin JJ, Vinod N, Min Y, Makita N, Bludau H, et al. Co-delivery of paclitaxel and cisplatin in poly(2-oxazoline) polymeric micelles: implications for drug loading, release, pharmacokinetics and outcome of ovarian and breast cancer treatments. *Biomaterials* 2019; **192**:1−14.
3. Seruga B, Ocana A, Tannock IF. Drug resistance in metastatic castration-resistant prostate cancer. *Nat Rev Clin Oncol* 2011;**8**: 12−23.
4. Kanamala MJ, Wilson WR, Yang M, Palmer BD, Wu Z. Mechanisms and biomaterials in pH-responsive tumour targeted drug delivery: a review. *Biomaterials* 2016;**85**:152−67.
5. Edgar PH, Alberto FM. Advanced targeted therapies in cancer: drug nanocarriers, the future of chemotherapy. *Eur J Pharm Biopharm* 2015;**93**:52−79.
6. Shi J, Kantoff PW, Wooster R, Omid CF. Cancer nanomedicine: progress, challenges and opportunities. *Nat Rev Cancer* 2017;**17**: 20−37.
7. Luo C, Sun J, Sun BJ, He ZG. Prodrug-based nanoparticulate drug delivery strategies for cancer therapy. *Trends Pharmacol Sci* 2014;**35**: 556−66.
8. Yang C, Tu K, Gao H, Zhang L, Sun Y, Yang T, et al. The novel platinum (IV) prodrug with self-assembly property and structure-transformable character against triple-negative breast cancer. *Biomaterials* 2019;**232**:11975.
9. Sykes EA, Dai Q, Sarsons CD, Chen J, Rocheleau JV, Hwang DM, et al. Tailoring nanoparticle designs to target cancer based on tumor pathophysiology. *Proc Natl Acad Sci Unit States Am* 2016;**113**: E1142−51.
10. Saito G, Swanson JA, Lee KD. Drug delivery strategy utilizing conjugation *via* reversible disulfide linkages: role and site of cellular reducing activities. *Adv Drug Delivery Dev* 2003;**55**: 199−215.
11. Mayr J, Heffeter P, Groza D, Galvez L, Koellensperger G, Roller A, et al. An albumin-based tumor-targeted oxaliplatin prodrug with distinctly improved anticancer activity. *Chem Sci* 2017;**8**:2241−50.
12. Luo C, Sun J, Sun BJ, Liu DC, Miao L, Goodwin TJ, et al. Facile fabrication of tumor redox-sensitive nanoassemblies of small-molecule oleate prodrug as potent chemotherapeutic nanomedicine. *Small* 2016;**12**:6353−62.
13. Sleep D. Albumin and its application in drug delivery. *Expet Opin Drug Deliv* 2015;**12**:793−812.
14. Li ZB, Wang YQ, Zhu JJ, Zhang YC, Zhang WJ, Zhou M, et al. Emerging well-tailored nanoparticulate delivery system based on *in situ* regulation of the protein corona. *J Control Release* 2020;**320**: 1−18.
15. Wei W, Luo C, Yang JC, Sun BJ, Zhao DY, Liu Y, et al. Precisely albumin-hitchhiking tumor cell-activated reduction/oxidation-responsive docetaxel prodrugs for the hyperselective treatment of breast cancer. *J Control Release* 2018;**285**:187−99.
16. Zhang D, Yang JC, Guan JB, Yang B, Zhang SW, Sun MC, et al. *In vivo* tailor-made protein corona of a prodrug-based nano-assembly fabricated by redox dual-sensitive paclitaxel prodrug for the superselective treatment of breast cancer. *Biomater Sci* 2018;**6**: 2360−74.
17. Li XS, Yu S, Lee Y, Guo T, Kwon N, Lee D, et al. *In vivo* albumin traps photosensitizer monomers from self-assembled phthalocyanine nanovesicles: a facile and switchable theranostic approach. *J Am Chem Soc* 2018;**141**:1366−72.
18. Zhang FW, Zhu GZ, Jacobson O, Liu Y, Chen K, Yu GC, et al. Transformative nanomedicine of an amphiphilic camptothecin prodrug for long circulation and high tumor uptake in cancer therapy. *ACS Nano* 2017;**11**:8838−48.